Chapter 2 Direct Simulation of Ground-Water Age

2.1 Introduction

The age of water in a groundwater system is useful for quantitative analysis. Various environmental tracers can be used to estimate the time since recharge for groundwater samples collected from various locations. These age data can be used in turn to constrain the parameters of models of flow and transport. Isotopic information is typically interpreted by using a travel time approach, simulating groundwater movement as 'piston' flow. Reilly and others (1994) show that an advective model of groundwater age, simulated by numerical particle tracking, is consistent with the distribution of chlorofluorocarbons and tritium observed in a shallow sand and gravel aquifer. In the advective model, the age is determined by the travel time of water, computed from Darcy's law. However, isotope transport in groundwater is often not by advection alone.

Several studies have indicated that estimates of groundwater travel time can be in error if the effects of dispersion and mixing on isotope concentrations are ignored. Plummer and others (1993, p. 287) give an overview of current methods for age-dating groundwater, and point out, as have many others, that "Because environmental tracers are dissolved solutes which are transported along with the ground water, it is usually necessary to consider effects of hydrodynamic dispersion on the modeled age." Walker and Cook (1991, p. 41) "show how neglecting diffusion can lead to serious underestimates of groundwater ages in unconfined aquifers where recharge rates are similarly low" when using the isotope carbon-14. Maloszewski and Zuber (1991) demonstrate the effects of matrix diffusion and exchange reactions on carbon-14 movement in fractured rocks and on groundwater age. Geyh and Backhaus (1978)

examine the effects of diffusion and mixing during pumping on carbon-14 distribution and age. The diffusion of carbon-14 from a confined aquifer into adjacent aquitards, and the resulting effect on interpreted ages, is quantified by Sudicky and Frind (1981). In their review, Mazor and Nativ (1992, p. 211) identify "problem areas" in the interpretation of groundwater age, including "lack of single recharge and discharge areas; . . . entrapment of ground water in 'dead' volumes . . .; (and) mixing of ground water of various ages."

Incorporation of the effects of transport processes other than advection allows additional information to be extracted from tracer distributions. For example, Torgersen and others (1978) estimate vertical diffusivity from observed tritium/helium-3 distributions in lakes. Weeks and others (1982) used fluorocarbon distribution in the unsaturated zone to estimate soil diffusion coefficients. A model of age that incorporates dispersion can be helpful in identifying the dispersive properties of the groundwater system (Robinson and Tester, 1984), in addition to the mean flow properties. Egboka and others (1983) estimate longitudinal dispersivity from the observed tritium distribution by fitting a one-dimensional model of tritium transport. Musgrove and Banner (1993) use isotopic information to help quantify mixing of distinct saline waters in a regional scale flow system.

The effects of diffusion, dispersion, and mixing can be incorporated in a transport simulation of the tracer or tracers of interest, for example tritium (Nir, 1964; Simpkins and Bradbury, 1992; Solomon, et al., 1993). Tritium is an isotope of hydrogen that is incorporated in water molecules. Simulation of tritium transport by use of a model that accounts for dispersion and diffusion reflects the underlying dispersion and diffusion of water molecules, and these water molecules have different ages. Thus, the age of the water *itself* is affected by diffusion, dispersion, and other hydrodynamic processes.

In the same way that particle tracking is used to generate groundwater age for the case of advection alone, simulation of groundwater age as affected by dispersion and

mixing, without resort to separate models for separate tracers, can be useful. Such an analysis complements, but does not replace, simulation of transport of the tracer of interest, which can be affected by processes, such as sorption and chemical exchange (Fritz et al. 1979), that do not affect the water.

The concept of a residence-time distribution has been used for many years to describe the statistics of the lifetimes of components in a flowing reactor (MacMullin and Weber, 1935; Danckwerts, 1953). This approach is chosen because molecules do not behave identically, rather mixing, diffusion, and variability in flow conditions result in different paths and residence times for different molecules. Residence-time distributions have been widely applied to the analysis of chemical reaction systems (Levenspiel, 1972). Eriksson (1958), Bolin and Rodhe (1973), and Nir and Lewis (1975) discuss the application of residence-time-distribution theory to steady and transient geophysical systems. Robinson and Tester (1984) use residence-time distributions determined from tracer tests to analyze dispersion in a fractured geothermal reservoir. Campana and Simpson (1984) apply some of these concepts to isotopic age dating of groundwater with a discrete-state (as opposed to continuous-state) compartment model in which separate areas of the groundwater system are treated as mixed reservoirs.

The underlying connection between the residence-time distribution and transport of an ideal tracer can be exploited to develop residence-time distributions corresponding to solutions of the advection-dispersion transport equation (Danckwerts, 1953; Wen and Fan, 1975; Nauman, 1981; Zuber, 1986). Danckwerts (1953) describes how the residence-time distribution can be determined experimentally from the outflow concentration of a nonreactive tracer. In this context, the mean age at a point, determined from temporal integrals of the concentration (described below), is affected by all of the processes accounted for in the solute-transport equation, including dispersion and mixing. The connection between resident concentration and probabilistic travel-time approaches to simulating groundwater transport is described by Shapiro and Cvetkovic (1988) and by

Dagan and Nguyen (1989), who discuss advantages of the travel-time approach for some analyses. Recently, Harvey and Gorelick (1995) present a general framework for application of temporal moment-generating equations to reactive transport.

It is shown in this chapter that the distribution of groundwater age obeys a special form of the solute-transport equation. The mean age can be simulated directly in an analytical or numerical transport model and the result of the simulation—that is, the predicted 'concentration'—is the mean age. This spatial age distribution is obtained directly, without further manipulation external to the transport simulation. For steady-state flow conditions, the age transport equation is derived from previous results on the residence-time distribution in systems governed by the advection-dispersion equation. This form has been presented previously for analysis of mean or 'local' age of air in a room during ventilation (Sandberg, 1981). A more general derivation here for transient flow conditions is based on the assumption of conservation of imaginary 'age mass.' This derivation also incorporates exchange processes; this framework is used to examine the impact of matrix diffusion on steady-state age. The method is illustrated by several example simulations, including cases representative of mildly-heterogeneous porous media and highly-heterogeneous fractured rock.

2.2 Derivation of Mean-Age Transport Equation

2.2.1 Residence-Time Distribution

Danckwerts (1953) defined a function C(t) to characterize the residence-time distribution for molecules in a chemical reactor. This function corresponds to the concentration at the reactor exit of a solute that is injected as an impulse (unit mass in an infinitely small time period) at the reactor entrance at time zero. For one-dimensional piston flow (advection only) conditions, the function C(t) is zero except at the time equal to the advective travel time of the system, at which time the function is a Dirac delta. In the case of complete mixing, C(t) is an exponentially decaying function; the outflow concentration is equal to the uniform concentration within the reservoir, which decreases because of the addition of tracer-free fluid at the inflow. For transport in porous media, the function C is analogous to the outflow mass flux (mass per unit time) of a column, that is c, the concentration measured in flux (Kreft and Zuber, 1978). In multi-dimensional systems, the mass injected on all inflow boundaries is proportional to the fluid flux across the boundary. Levenspiel (1972) and Wen and Fan (1975) present several models for transport in flowing reactors and their respective C functions.

The mean residence time in a steady-flow domain can be determined from the concentration of a tracer injected as an impulse at time zero as:

$$A = \frac{\int_0^\infty t\,c\,dt}{\int_0^\infty c\,dt} = \frac{E}{M} \qquad (2.1)$$

where A is the mean residence time, or the mean age of molecules, in the reactor (Spalding, 1958). The numerator of (2.1) is a concentration-weighted average time,

which I will denote as E. This form is similar to the expectation of a random variable t with probability density function c. The denominator normalizes the numerator such that c divided by the time integral of c has the properties of a probability density function. This integral, which is constant and uniform for steady flow (Spalding, 1958), will be denoted as M. This term is uniform for multi-dimensional systems provided the mass injected on inflow boundaries is proportional to fluid flux across the boundary (see Harvey and Gorelick, 1995).

For transport by advection and dispersion in a constant-density fluid, the concentration satisfies

$$\frac{\partial\, c\theta}{\partial t} = \nabla\bullet\theta\mathbf{D}\bullet\nabla c - \nabla\bullet\mathbf{q}c \tag{2.2}$$

where θ is the moisture content (porosity for saturated flow); **D** is the dispersion tensor; and **q** is the specific-discharge vector. A standard model of dispersion in groundwater is assumed such that the product of moisture content and the dispersion tensor, **D**, is given by

$$\theta D_{ij} = \left(\theta D_m + \alpha_T q\right)\delta_{ij} + \left(\alpha_L - \alpha_T\right)\frac{q_i q_j}{q} \tag{2.3}$$

where D_m is the diffusion coefficient; the Kronecker delta is $\delta_{ij} = 1$ if $i=j$ and $\delta_{ij} = 0$ if $i\neq j$; α_L and α_T are, respectively, the longitudinal and transverse dispersivities; q_i is a component of the specific discharge vector; and q is the magnitude of specific discharge. Multiplying (2.2) by time and integrating through all time gives (Spalding, 1958):

$$-\theta M = \nabla\bullet\theta\mathbf{D}\bullet\nabla E - \nabla\bullet\mathbf{q}E \quad . \tag{2.4}$$

The left side of (2.4) is obtained through integration by parts of the time derivative term. Dividing by M, which is uniform and can be brought inside the spatial derivatives, and assuming porosity is also uniform, gives

$$\nabla \cdot \mathbf{D} \cdot \nabla A - \frac{1}{\theta} \nabla \cdot \mathbf{q} A + 1 = 0 \qquad (2.5)$$

where the defined mean age A = E / M has been substituted (see Sandberg, 1981, for comparison). Thus, the mean age at a point satisfies a steady-state advection-dispersion transport equation with an internal source of unit (1) strength. A more general form of (2.5) is derived in the next section by assuming that age is conserved under mixing. This derivation also leads to natural choices for boundary conditions for (2.5) to complete the mathematical framework.

Computing age by particle tracking corresponds to solution of (2.5) without the dispersion term. In this case, particle paths are defined by the characteristics of the governing equation and the increasing travel time corresponds to the unit source in (2.5). Equation (2.1) can be used to calculate mean age within a small volume from a particle tracking analysis to include, for example, the mixing induced by sampling. The methods presented here for age simulation also may be useful in accounting for the effects of dispersion and mixing on other analyses involving groundwater and travel time such as contamination from landfills (Lee and Kitanidis, 1993) and time-dependent capture zones (Bair et al., 1990).

2.2.2 Conservation of Age Mass

In this section, a more general form of the age transport equation is derived from mass-conservation principles. Assuming that the mean age of mixed waters is a mass-weighted average, then the mean age is analogous to a conservative solute concentration. Although age is not a directly-measurable physical property, and thus this assumption

cannot be verified experimentally, it seems suitable for our conceptual model that when two water masses are mixed, the mean age of the mixture is the mass-weighted average age of the mixed components. It may be possible to experimentally verify this assumption using a tracer that has an input function that varies linearly with time. A given mass of water with a mean age A can be assumed to be characterized by its 'age mass,' the product of the mean age and the water mass, $A \rho V$, where ρ is water density and V is water volume. Assuming that the density of the water is constant, the mean age of a two-component mixture is a volume-weighted average:

$$A = \frac{A_1 V_1 + A_2 V_2}{V_1 + V_2} \tag{2.6}$$

where the subscripts distinguish the components. This is completely analogous to the concentration of a conservative solute under mixing in constant-density water. This analog can be exploited to derive a governing transport equation for mean age.

A governing equation for age-mass transport can be derived from a simple box balance similar to the derivation of the mass-transport equation by Konikow and Grove (1977; see also Bear, 1979). Consider conservation of age mass in a control volume (dimensions Δx by Δy by Δz) of aquifer material. The age mass within the control volume is the product of the age (A) and the mass of water, $\theta \rho \Delta x \Delta y \Delta z$. The age-mass flux (per unit area) across the boundaries of the control volume is designated **J**, with components J_x, J_y, and J_z, and includes advection with the water as well as dispersive flux. Over a time step of length Δt, the age mass of the water initially in the control volume increases by the product of Δt and the mass of water. Additionally, an internal net source of age mass of rate F is included to account for, for example, net exchange of age mass with separate phases. Physical processes included in F are described below. Assuming that the age mass is conserved, a difference form of a conservation equation is

$$A(t+\Delta t)\,\theta\,\rho\,\Delta x\,\Delta y\,\Delta z = A(t)\,\theta\,\rho\,\Delta x\,\Delta y\,\Delta z + \Delta t\,\theta\,\rho\,\Delta x\,\Delta y\,\Delta z +$$

$$\Delta t\Big\{\Delta y\,\Delta z\big[J_x(-\Delta x/2) - J_x(+\Delta x/2)\big] + \Delta x\,\Delta z\big[J_y(-\Delta y/2) - J_y(+\Delta y/2)\big] + \qquad (2.7)$$

$$\Delta x\,\Delta y\big[J_z(-\Delta z/2) - J_z(+\Delta z/2)\big]\Big\} + F\,\Delta t\,\Delta x\,\Delta y\,\Delta z \quad .$$

Dividing by the volume and the time-step length, and allowing the size of the control volume and the time-step length to go to zero in the limit gives the governing partial differential equation for mean-age transport:

$$\frac{\partial A\theta\rho}{\partial t} = \theta\rho - \frac{\partial J_x}{\partial x} - \frac{\partial J_y}{\partial y} - \frac{\partial J_z}{\partial z} + F$$

$$= \theta\rho - \nabla\bullet\mathbf{J} + F \quad . \qquad (2.8)$$

This form of the mean-age transport equation is more general than (2.5) in that the water density is allowed to vary, the model of dispersive flux is not specified, and the equation is transient. The mean age spatial distribution can be determined from (2.8) even for aquifer systems with unsteady flow, provided the flow history is known. The ability to simulate the transient evolution of groundwater age may be useful, for example, in assessing the impact of climate change on large aquifer systems.

To complete the governing equation, a description of dispersive age-mass flux in terms of age, or its gradient, is needed. Here, I adopt the standard model of mass flux such that **J** is composed of advection, diffusion, and dispersion modeled as Fickian diffusion. That is, **J** in (2.8) is replaced by

$$\mathbf{J} \approx A\,\rho\,\mathbf{q} - \theta\rho\mathbf{D}\bullet\nabla A \qquad (2.9)$$

where **D** is the dispersion tensor and includes a diffusion term. By substitution, the governing equation becomes

$$\frac{\partial A\theta\rho}{\partial t} = \theta\rho - \nabla\bullet A\rho\mathbf{q} + \nabla\bullet\theta\rho\mathbf{D}\bullet\nabla A + F \quad . \tag{2.10}$$

If the porosity and density are constant in time and uniform in space, (2.10) becomes

$$\frac{\partial A}{\partial t} = 1 - \nabla\bullet A\frac{\mathbf{q}}{\theta} + \nabla\bullet\mathbf{D}\bullet\nabla A + \frac{F}{\theta\rho} \quad . \tag{2.11}$$

Under steady flow conditions the time derivative in (2.11) (or (2.10)) can be set to zero to derive a governing equation for steady-state mean-age spatial distribution. A steady-state age distribution does not exist if both **q** and **D** are zero. The steady-state equation derived from (2.11) is the same as (2.5) derived above from residence-time distribution theory, with an additional source term F, which is discussed below. Initial and boundary conditions for the mean-age transport equation can be specified from the control-volume balance.

2.2.3 Boundary and initial conditions

The age of groundwater is relative to the time at which the water entered the system. That is, recharge to the system is assumed to have age zero. From the definition of age mass, the age-mass flux, the product of age and water-mass flux, is also zero at all inflow boundaries. Furthermore, the age-mass flux across all no flow boundaries is also zero. These conditions can be written as:

$$\mathbf{J}|_{\Gamma_1}\bullet\mathbf{n} = 0 \tag{2.12}$$

where Γ_1 is a noflow or inflow boundary and **n** is its unit outward normal. Note that (2.12) uses the previous notation for total age-mass flux, **J**, which includes dispersion as well as advection. Thus, no dispersion is assumed to occur upstream across the boundary against the direction of the incoming flow.

The boundary condition on outflow boundaries depends on the physical situation. A common assumption, which I will adopt here, is that mass flux across an outflow boundary occurs only by advection. This condition of no dispersion across the boundary can be written

$$\mathbf{D}\,\nabla A\big|_{\Gamma_2} \bullet \mathbf{n} = 0 \qquad (2.13)$$

where Γ_2 is the outflow boundary. This condition probably is most appropriate for discharge to surface-water bodies. Alternate boundary conditions for other physical situations, such as advection and dispersion into a separate aquifer outside of the simulation domain, also can be formulated, but they are not pursued here.

The general form of the governing equation for mean age transport is transient. If the flow field is steady, then the steady distribution of mean age is determined by solution of the steady-state form of the governing equation, similar to (2.5). In this case, an initial condition is not required. If the flow field is not steady, then the transient form of the governing equation for age transport must be used and an initial condition is required. That is, the initial mean age at every point within the aquifer system must be specified. For simulation times that are very long, relative to the rate of advection through the aquifer system, the groundwater age is insensitive to the initial age distribution, although the initial age is required mathematically to yield a solution.

2.2.4 Internal source of age mass

The internal net source of age mass, F, can account for several processes. Many aquifer systems are modeled in only the horizontal dimensions because vertical head gradients and flow rates are assumed to be small. A governing equation for this case can be obtained from (2.5) or (2.11) by vertical integration across the saturated thickness. In the resulting two-dimensional model, F could include the age-mass flux due to inflow from an underlying hydrogeologic unit. For example, for the case of leakage through an aquitard, F would be the product of the leakage water mass flux rate and the age of the leakage, and would be positive for the case of inflow to the aquifer of interest. Similarly, evapotranspiration from a two-dimensional horizontal model would be treated as a net sink of age mass and F would be negative.

The internal sink/source term F could represent age-mass exchange between phases, for exmaple during unsaturated flow through partially frozen soil. In this case, some of the flowing water may freeze, acting as a sink for age mass, or stationary ice of a different age may melt, acting as a source of age mass for the flow system. Of course, as with the other examples, for the case of age-mass sources such as melting ice, the age of the source water must be specified or determined from a separate, possibly coupled, mathematical model.

For the general three-dimensional model, F could represent sources and sinks of age mass due to multi-continua exchange. For example, flow in fractured rock can be modeled as a two-domain system, with separate transport equations for high-permeability fractures and for the rock matrix. Exchange of water between the fractures and the rock matrix would include an exchange of age mass. For the fracture domain, F would be the product of the rate of water-mass inflow from the matrix and the age of that water. The F term for the rock-matrix equation would be of equal magnitude but opposite in sign.

Low-flow or stagnant zones are not necessarily included in this internal source term, but can be handled directly in the governing equation. In such zones, the advective

flux is small and the groundwater age is determined primarily by diffusion, which is included in the dispersion tensor **D**. In the absence of diffusion, the age of water at a stagnation point in a steady flow field is by definition infinite. However, this infinite age applies only to a point which has infinitesimally small fluid volume.

2.2.5 Effect of matrix diffusion at steady state

The age-mass concept can be used to evaluate the effect of matrix diffusion on steady-state age distribution. Consider age-mass transport in a fractured rock system which is modeled as advection and dispersion in a continuum of connected fractures, coupled with diffusion to and from the rock matrix. In this case, F represents the rate of age-mass transfer between the rock matrix and the fractures. Hence, F appears as the boundary flux for an equation governing age-mass transport within the rock matrix. In general, the solution of this problem would require solution of two coupled transport equations. However, for the case of steady-state age distribution, F can be computed directly.

Under steady-state conditions, an integrated age-mass conservation equation for the rock matrix has only three components: (1) accumulation of age-mass (zero for steady state), (2) boundary flux, and (3) production of age-mass by aging. Because (1) is zero in steady state, (2) and (3) must balance. Hence, the net boundary flux F of age-mass out of the rock matrix into the fracture is equal to the total age-mass production rate in the matrix, which is the product of the rock porosity and the water density in the rock matrix Hence, at steady state (2.10) can be written

$$0 = \theta\rho - \nabla\bullet A\rho\mathbf{q} + \nabla\bullet\theta\rho\mathbf{D}\bullet\nabla A + \theta_m\rho_m \quad , \qquad (2.14)$$

where θ_m is the bulk porosity of the rock matrix and ρ_m is the density of water in the matrix. In this case, the porosity of fracture system (θ) is the bulk fracture porosity: the

total volume of the fractures per unit volume of aquifer. Assuming that the density of water is constant, and that both fracture and rock porosities are uniform, (2.14) can be simplified to:

$$0 = 1 - \nabla \bullet A \frac{\mathbf{q}}{\theta + \theta_m} + \frac{1}{\theta + \theta_m} \nabla \bullet \theta \mathbf{D} \bullet \nabla A \quad . \tag{2.15}$$

Thus, the age distribution is identical to that of a single continuum system in which the porosity is the sum of the fracture and rock matrix porosities. The apparent velocity is 'retarded' compared to the velocity of water in the fractures alone, and the rate of dispersive spreading is likewise reduced by the total porosity. Of course, this analysis assumes that the age distribution is in steady state. Because of the slow rate of diffusion in rock, disequilibrium between the age-mass production in the rock and diffusion out into the fracture may exist for millions of years.

2.3 Examples

2.3.1 Regional Flow in Cross Section

The mathematical theory for simulation of groundwater age developed in the previous section is applied to a regional model of groundwater flow and transport in cross-section. This application demonstrates the practical simulation of groundwater age distribution using the age transport equation, both with and without dispersion. The impact of heterogeneous hydraulic conductivity and porosity, and of matrix diffusion on age distributions are illustrated. Six hypothetical aquifer systems are considered:

- **uniform** aquifer with homogeneous hydraulic conductivity and porosity;
- **layered** aquifer in which a high-permeability layer exists at depth;
- **discontinuous layered** aquifer in which a high permeability layer at the aquifer bottom is discontinuous; in this case, the permeability contrast is 100:1;
- **stratified heterogeneous** aquifer in which several discontinuous horizontal high-permeability (100:1) zones occur at different depths; results are presented for uniform porosity and nonuniform porosity.

The uniform and layered configurations are similar to those analyzed by Freeze and Witherspoon (1967) in a landmark series of papers in which they used numerical flow models to study the characteristics of regional groundwater flow. The flow equation is solved using a block-centered finite-difference flow model, MODFLOW (McDonald and Harbaugh, 1988). A three-dimensional method-of-characteristics solute transport model, MOC3D (Goode and Konikow, 1991; Konikow and others, 1996), is modified to solve the age transport equation, including the zero-order source term for age in equation (2.10). In contrast to finite-difference or finite-element numerical solutions of the transport equation, MOC3D is well suited to the case of advection alone, $\mathbf{D}=\mathbf{0}$.

The domain geometry and boundary conditions are identical for the six hypothetical regional aquifers considered. The domain is 1 km long and 100 m thick.

Except where noted, this spatial domain is discretized by 10 rows in the vertical direction, each 10 m thick, and 50 columns in the horizontal direction, each 20 m long. Noflow boundary conditions are specified on the left, right, and bottom boundaries. The top boundary represents the water table and is modeled here with a combination of specified-flux and specified-head conditions. The change in the position of the domain boundary due to movement of the water table is considered to be a minor effect, and is ignored here.

The uniform and layered regional flow systems modeled here are similar to those considered by Freeze and Witherspoon (1967), but a different water-table boundary condition is used. Freeze and Witherspoon (1967) used numerical flow models to study the effects of nonuniform hydraulic conductivity on regional groundwater flow. As previously noted by Freeze and Cherry (1979, p. 204), the results obtained by Freeze and Witherspoon (1967) were affected by the choice of specified-head boundary conditions along the entire water table, the top boundary of the flow domain. With this approach, variations in subsurface permeability lead to significant changes in recharge magnitude and distribution, without affecting water-table altitudes. For the simulations here, I choose boundary conditions at the opposite extreme, where the recharge is modeled as a specified-flux boundary condition (fig. 2-1). In reality, both water-table altitudes and net groundwater recharge are sensitive to subsurface permeability. Specified-head conditions similar to those of Freeze and Witherspoon (1967) are used at discharge locations. Thus, water-table altitudes are free to change in response to various hydraulic-conductivity configurations, but the recharge distribution is identical in both cases. These simulations yield greater changes in hydraulic heads but smaller changes in flow rates compared to the simulations of Freeze and Witherspoon (1967).

The first two cases are identical except that in the layered case a high-permeability layer occurs at the aquifer bottom. The isotropic hydraulic conductivity of the homogeneous aquifer is $K_1 = 10^{-6}$ m/s and its porosity is 0.2. The hydraulic

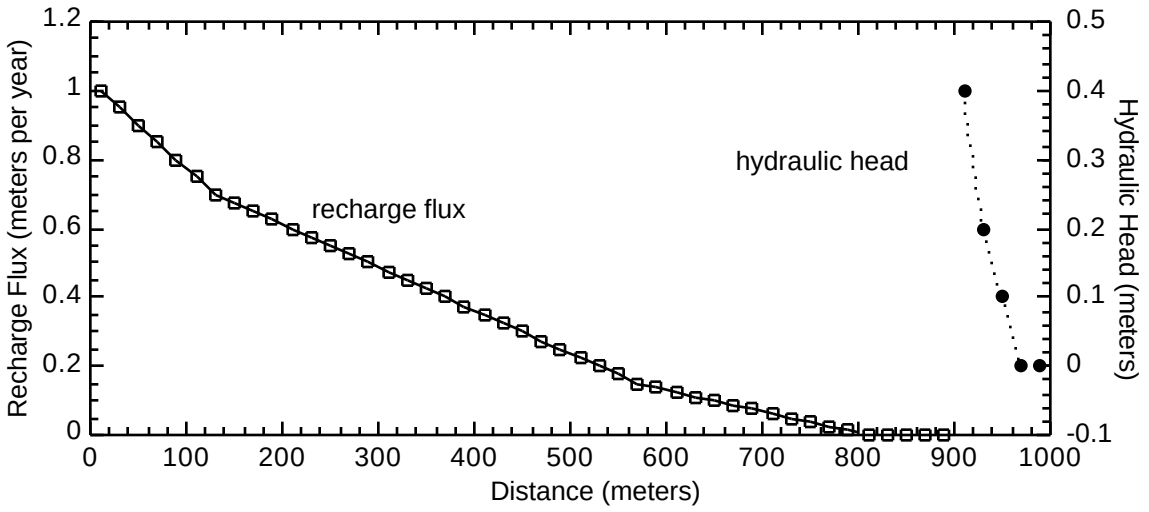

Figure 2-1 Flow boundary conditions on top of cross-sectional model of regional aquifer system showing specified-flux values for recharge nodes and specified-head values for discharge nodes.

conductivity of the layered aquifer system is the same in the upper 70 m of the system, but is ten times greater, $K_2 = 10 \times K_1 = 10^{-5}$ m/s, in the lower 30 m . The porosity is the same for both layers, 0.2.

Figures 2-2a and 2-3a show the head distribution and groundwater-flow velocities for steady-state conditions, and figures 2-2b and 2-3b show corresponding streamlines for the **uniform** and **layered** cases. The imposed boundary conditions and uniform properties lead to a smooth distribution of head and gradual variations in velocity for the uniform aquifer (fig. 2-2a). In the layered case, most flow occurs through the deep layer , where the hydraulic conductivity is greater (fig. 2-3a). Because the transmissivity is greater, water-table altitudes are lower in the layered than in the uniform case. Velocity changes abruptly at the interface in the layered case, yielding refracting streamlines (fig. 2-3b), that contrast with the smooth streamlines throughout the uniform aquifer (fig. 2-2b).

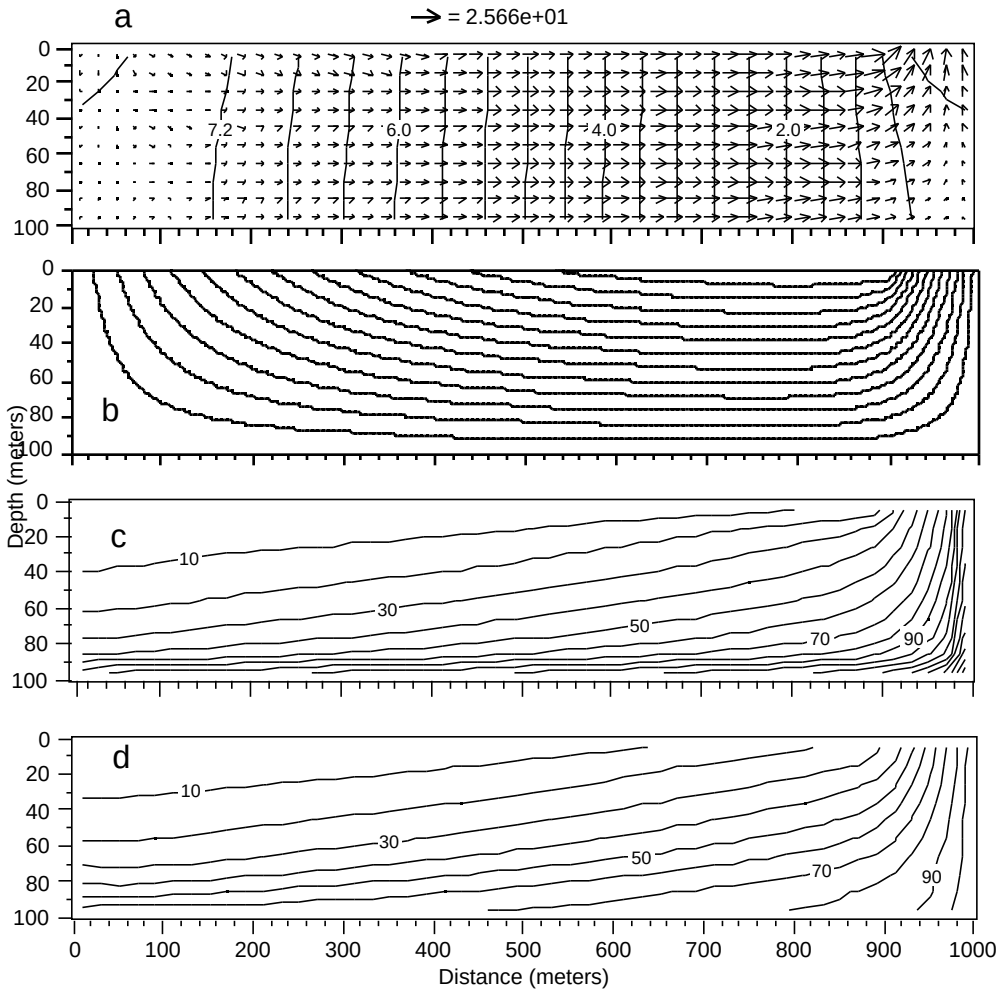

Figure 2-2 Results of direct simulation of groundwater age in a **uniform** regional aquifer system in which the hydraulic conductivity is 10^{-6} m/s: (a) Cross-sectional domain with hydraulic-head contours (0.4 m interval) and velocity vectors. Vertical exaggeration is 2X and the 10 row by 50 column finite-difference grid used for the numerical flow and transport solutions is indicated by the small ticks on each axis. (b) Streamlines from recharge to discharge locations. (c) Contours of simulated groundwater age for advection only ($D_m = \alpha_L = \alpha_T = 0$). Contour interval 10 years. (d) Contours of simulated groundwater age for advection and dispersion using $D_m = 1.16 \times 10^{-8}$ m^2/s, $\alpha_L = 6$ m, and $\alpha_T = 0.6$ m. Contour interval 10 years.

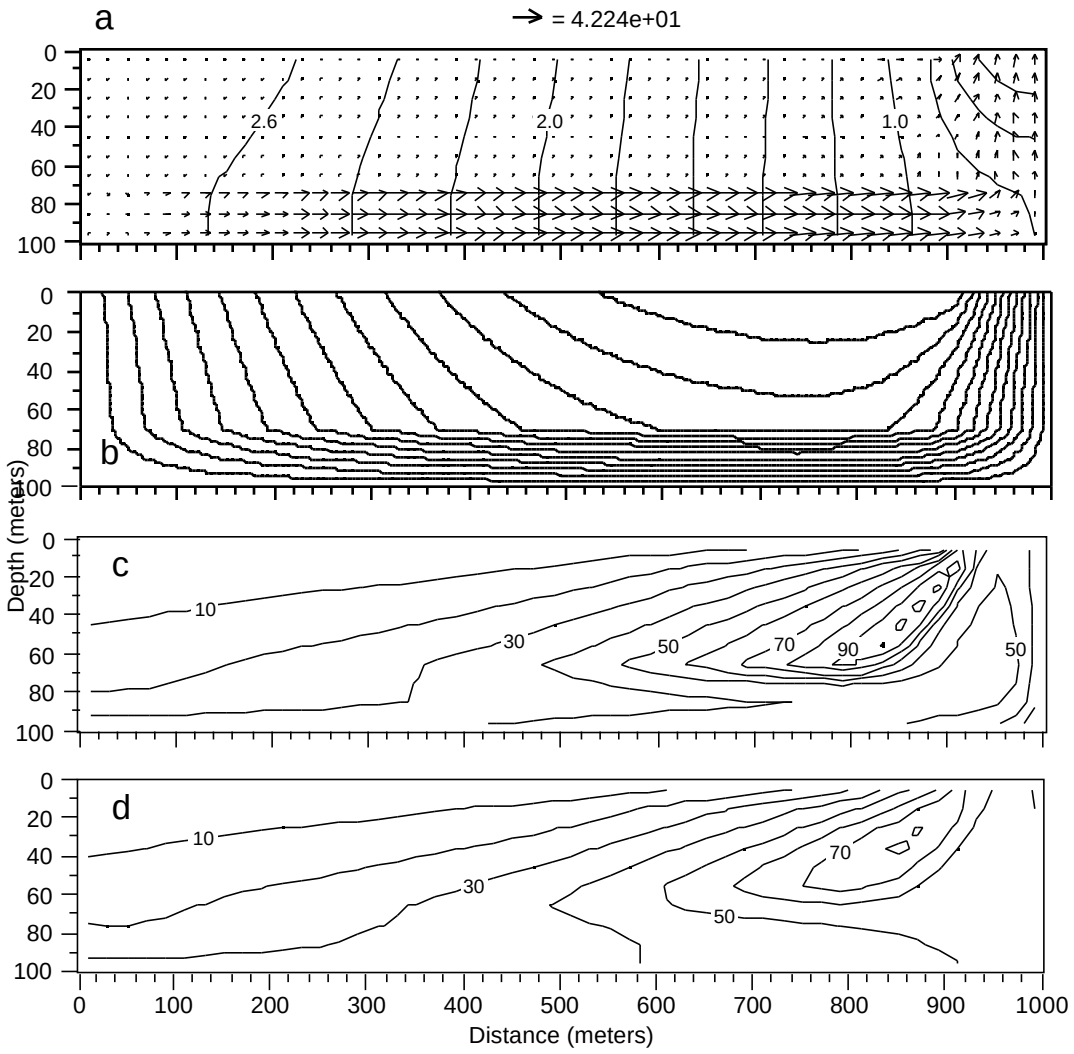

Figure 2-3 Results of direct simulation of groundwater age in a cross-section through a **layered** regional aquifer system in which the bottom layer is 30 m thick with hydraulic conductivity 10^{-5} m/s, and the overlying layer is 70 m thick with hydraulic conductivity 10^{-6} m/s: (a) Cross-sectional domain with hydraulic-head contours (0.2 m interval) and velocity vectors. Vertical exaggeration is 2X and the 10 row by 50 column finite-difference grid used for the numerical flow and transport solutions is indicated by the small ticks on each axis. (b) Streamlines from recharge to discharge locations. (c) Contours of simulated groundwater age for advection only ($D_m = \alpha_L = \alpha_T = 0$). Contour interval 10 years. (d) Contours of simulated groundwater age for advection and dispersion using $D_m = 1.16 \times 10^{-8}$ m^2/s, $\alpha_L = 6$ m, and $\alpha_T = 0.6$ m. Contour interval 10 years.

The groundwater age throughout the aquifer is readily simulated by solving the advection transport equation with the zero-order source term that accounts for aging (figs. 2-2c and 2-3c). For the uniform case, velocities are lowest along the no-flow boundaries on the left, bottom, and right. Along the right boundary, ages are the greatest at the bottom and decrease toward the discharge boundary at the top. Ages might be expected to increase continually toward the top of the right boundary, and this in fact occurs on individual streamlines. But the ages portrayed in Figures 2-2c and 2-3c are volume averages over 10 x 20 m cells. These cell-averaged values do not increase because converging streamlines near the discharge boundary bring younger water into the cells along the right boundary. That is, the maximum age at a point is at the top right corner of the domain, but the average age for the cell containing this point is less because of the convergence of streamlines in the cell.

The age distribution in the layered case is nonuniform and ages are greatest in the central part of the system, away from the boundaries (fig. 2-3c). Because the permeability of the lower layer is higher, the lowest velocities do not occur along the bottom of the system, but along the bottom of the upper layer. As with the homogeneous case, volume-averaged ages decrease toward the discharge boundary because the streamlines converge. The maximum water age in the layered aquifer system is about 90 years, whereas the maximum age in the uniform case is about 180 years. As discussed above, the total discharge through the aquifers is identical as a result of the specified-flux boundary conditions for recharge to the water table.

This result of greater maximum ages in the uniform case is highly dependent on aquifer structure and boundary-condition configuration. Simulation of a layered aquifer system identical to that shown here, but with the hydraulic conductivity of the lower layer decreased to 10^{-7} m/s, yields very different results. In this case, the upper portion of the system is more conductive than the lower and ages in the upper layer are similar to those in the homogeneous case. In the lower layer, however, flux and velocity are significantly

reduced because of the low permeability, and very old water is present, especially towards the right side of the domain. Maximum volume-average ages for this case, with advection alone, are more than 1,000 years.

The effect of dispersion on the groundwater age distribution is easily obtained by re-solving the transport equation and including dispersivities of α_L = 6 m and α_T = 0.6 m for the longitudinal and transverse components, respectively. In addition, a diffusion coefficient of $D_m = 1.16 \times 10^{-8}$ m^2/s is added to the dispersion tensor. This diffusion coefficient is about ten times higher than realistically expected values, and is used to illustrate the maximum likely effect of diffusion in these hypothetical aquifer systems. The effect of this diffusion alone is examined below.

Dispersive and diffusive mixing of water of different ages tends to limit the maximum ages (figs. 2-2d and 2-3d). Solute dispersive flux occurs, according to the generally accepted Fick's law model, in the direction of decreasing concentration. In complete analogy, the dispersive flux of age mass occurs in the direction of decreasing age, away from areas of maximum age. Where advective flux is relatively small—that is, where velocity is small—the effect of this dispersive flux on age distribution is greatest. The effect of longitudinal dispersion is mitigated in the case of age transport because, along a streamline, age increases smoothly in the direction of flow due to aging. Thus the steep longitudinal gradients typically associated with an advancing solute front are not present. However, steep gradients in age are present transverse to the flow direction, particularly in the layered case (figs. 2-3c and 2-3d). In these areas of steep gradients dispersion can have the greatest effect on groundwater age. Figure 2-4 is a contour map of the percent change in groundwater age, ranging from -37 to +64 percent, due to diffusion and dispersion for the layered case.

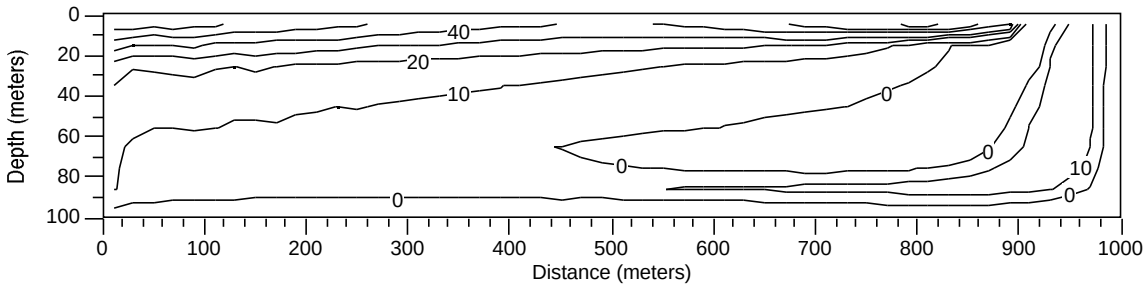

Figure 2-4 Percent difference in simulated age distribution between advection only and advection-dispersion (D_m = 1.16 x 10^{-8} m^2/s, α_L = 6 m, α_T = 0.6 m) cases in a **layered** regional aquifer system. The percent difference in simulated age ranges from -37 to +64 percent.

To examine further the relative contribution of diffusion and dispersion to the previous results, and to compare the theory developed here with residence-time-distribution (particle tracking) methods, a simulation of the layered case is conducted with advection and diffusion, but without dispersion. Figure 2-5 shows the results obtained by the theory proposed here, which are similar to those for advection alone, but exhibit a slight reduction in maximum ages. In the bottom layer, where velocities are high, diffusion has no observable effect on age distribution. Figure 2-5 also shows results of a particle-tracking model applied to the same problem. Particle paths and travel times are computed by linear velocity interpolation (Goode, 1990) and a random walk (Kinzelbach, 1988) to simulate diffusion. The groundwater age distribution is computed by numerical integration of equation (2.1). The close agreement between results obtained by using these alternative methods further supports the theoretical arguments presented in section 2.2.

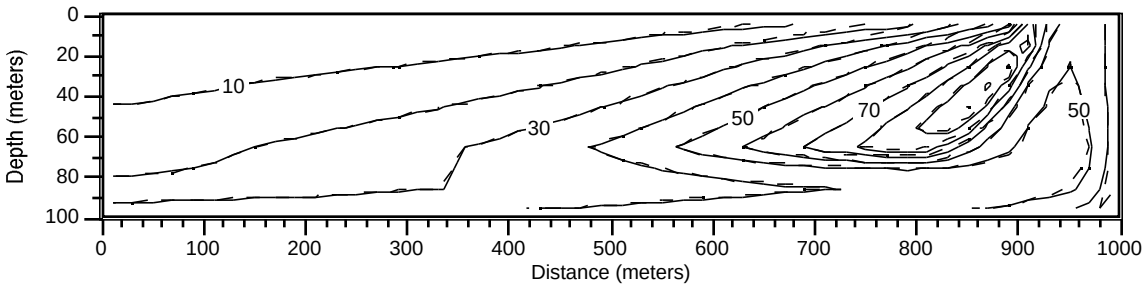

Figure 2-5 Contours of simulated groundwater age in a **layered** regional aquifer system for advection and diffusion obtained by using proposed transport equation method (solid lines), and by using a particle tracking and random walk method (dashed lines). The diffusion coefficient is 1.16×10^{-8} m^2/s and the contour interval is 10 years.

The **discontinuous layered** case is derived from the layered case but has a discontinuous bottom layer of even higher permeability. Here the high-permeability layer occurs only across part of the regional flow system in three sections. The bottom 30 m of the aquifer system has hydraulic conductivity $K_3 = 100 \times K_1 = 10^{-4}$ m/s in zones between 0-200 m, 400-600 m, and 800-1000 m distance from the left. The hydraulic conductivity is the same as the uniform case, $K_1 = 10^{-6}$ m/s, in the rest of the aquifer. The same value of porosity is used throughout the aquifer system, 0.2.

Flow is significantly diverted into the discontinuous high-permeability zones because of the 100 fold higher permeability (fig. 2-6a). The flow system is characterized by downward flow in the areas upgradient of and over the high-permeability zones, and upward flow at the downgradient end.

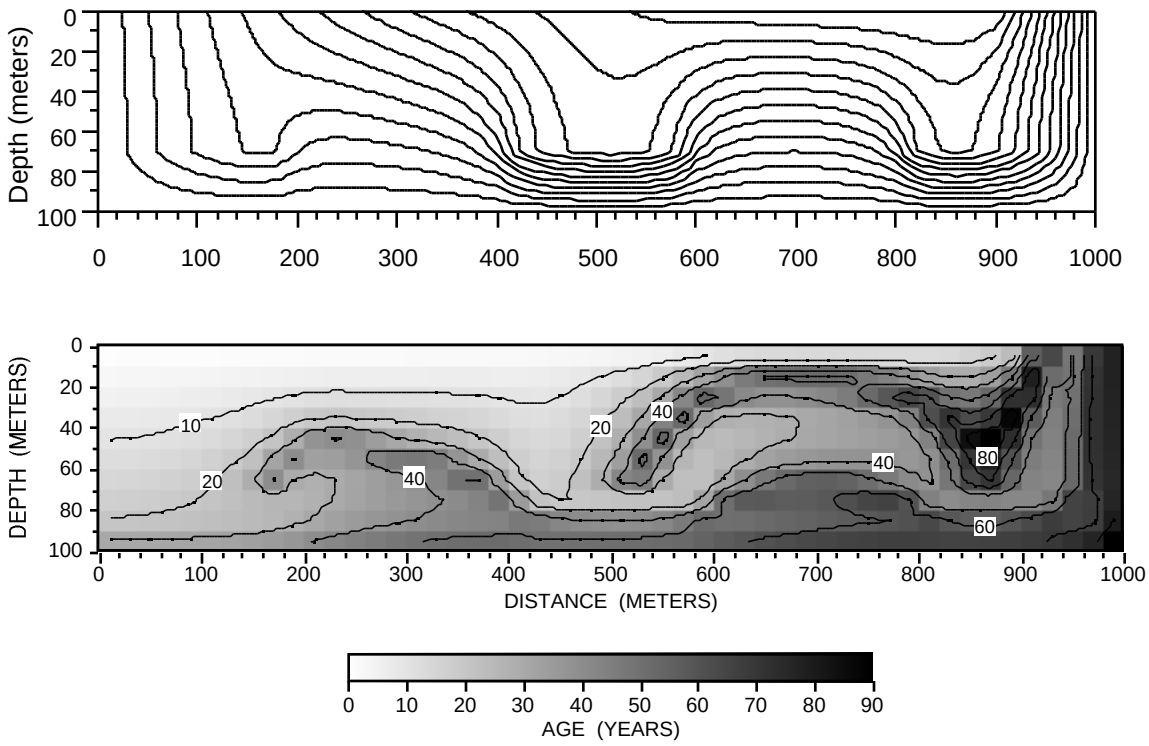

Figure 2-6 Results of direct simulation of groundwater age in a cross-section through a **discontinuous layered** regional aquifer system in which three high-permeability zones occur at the bottom. Each zone is 30 m thick with hydraulic conductivity 10^{-4} m/s and the horizontal extents are between 0 - 200 m, 400 - 600 m, and 800 - 1000 m from the left boundary. The remainder of the aquifer system has hydraulic conductivity 10^{-6} m/s. (a) Streamlines from recharge to discharge locations. Vertical exaggeration is 2X and the 10 row by 50 column finite-difference grid used for the numerical flow and transport solutions is indicated by the small ticks on each axis. (b) Contours of simulated groundwater age for advection only ($D_m = \alpha_L = \alpha_T = 0$). Contour interval 10 years.

The pattern of ages from advection alone is complex, even for this relatively simple case with only three high-permeability zones. As shown in Figure 2-6b, the nonuniform permeability distribution leads to widely varying travel times. As in the layered case, low horizontal velocities occur immediately adjacent to the high-permeability zones because their presence significantly reduces the local hydraulic

gradient. Hence, ground-water ages change significantly between adjacent flow lines depending on their history - whether they pass into high-permeability zones or pass through low-velocity areas adjacent to high-permeability zones.

The **stratified heterogeneous** case has several discontinuous high-permeability zones at different depths. The bulk of the aquifer has $K_1=10^{-6}$ m/s. Several very high permeability features are included; these features have $K_3 = 100\ K_1 = 10^{-4}$ m/s. The porosity is uniform, $\theta=0.2$. The two-order-of magnitude contrast in hydraulic conductivity causes a very complex flow pattern. Much of the horizontal flow occurs within the horizontal high-permeability features (fig. 2-7a). However, these features do not connect with each other, or with the top boundary. Outside of the high-permeability features, flow is primarily vertical, either between separate high-K zones, or between the upper high-K zones and the recharge/discharge boundaries at the top.

Although ages generally increase from left to right, in the direction of the overall flow, the age distribution is so complex that interpretation of the ages alone would be difficult (fig. 2-7b). For example, several closed contours of ages less than 40 years occur for $600 \leq x \leq 1000$ m. As with the layered case above, these closed contours occur because of the averaging of ages in model cells. Within high-K zones, the age is an average of many streamlines, some of which are very old. As these streamlines diverge downstream of the high-K zone, the youngest streamlines occupy cells in which no very-old streamlines occur, yielding younger cell-average ages. Conceptually, the cell-average age may represent the age of a sample taken from that location that mixed waters from the entire cell space, rather than the age at a point. This particular configuration yields youngest average ages outside the high-K zones, which is somewhat counter-intuitive. However, the occurrence of the oldest waters beneath the lower high-K zones re-emphasizes the shadowing effect of high-permeability features which reduce gradients in surrounding low-K areas.

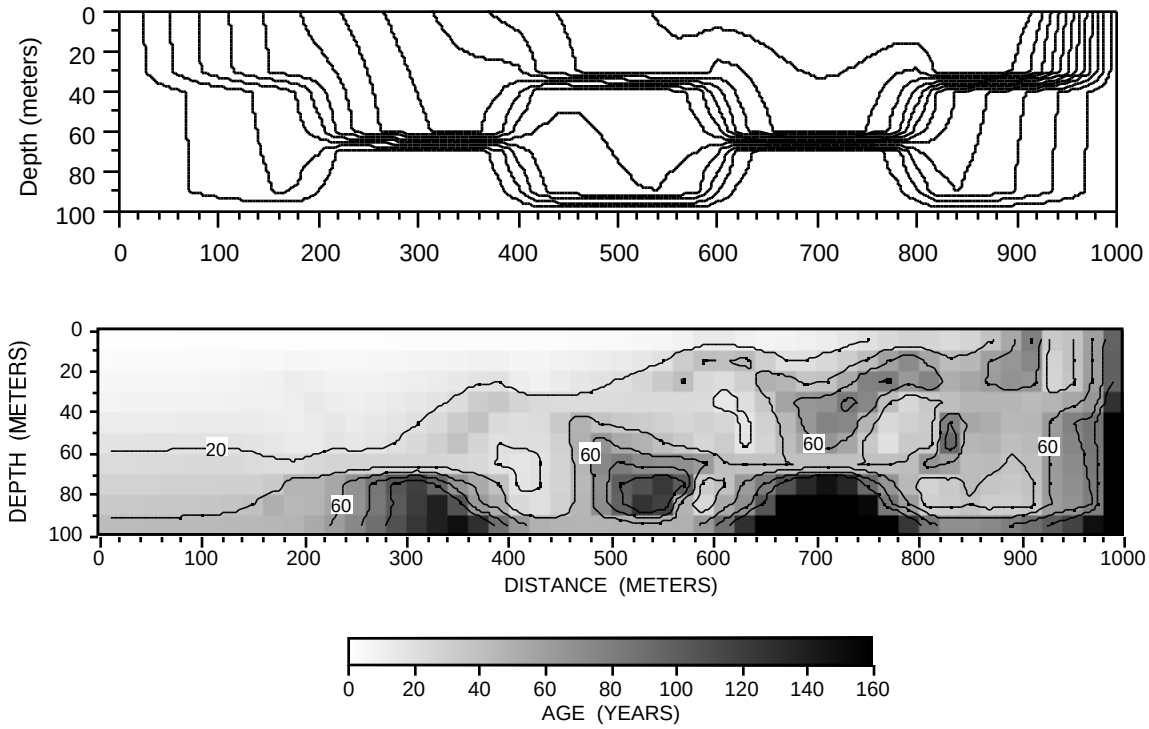

Figure 2-7 Results of direct simulation of groundwater age in a cross-section through a **stratified heterogeneous** regional aquifer system in which eight discontinuous high-permeability zones occur at three different depths. Each zone is 30 m thick with hydraulic conductivity 10^{-4} m/s and with horizontal extent of 200 m. The remainder of the aquifer system has hydraulic conductivity 10^{-6} m/s. Porosity is uniform, θ=0.2. (a) Streamlines from recharge to discharge locations. Vertical exaggeration is 2X and the 10 row by 50 column finite-difference grid used for the numerical flow and transport solutions is indicated by the small ticks on each axis. (b) Contours of simulated groundwater age for advection only ($D_m = \alpha_L = \alpha_T = 0$). Contour interval 10 years.

The second **stratified heterogeneous** case is derived from the previous case by changing the porosity of the lower 90 m of the system to θ_2=0.01. The hydraulic conductivity distribution is the same as the previous case, so the head gradients and fluxes are the same, but the velocity is increased by a factor of 20 in the lower part of the aquifer. This case illustrates the effect of stratified porosity; here the upper zone may represent a weathered rock zone with high porosity, and the lower zone may represent

unweathered rock with both highly-fractured and less-fractured zones. The ages in the fractured rock are lower than the previous case because of the reduced porosity, although the pattern of age variability is similar in many respects. However, the 20X large porosity in the overburden layer causes ages to be highest at the top of the system where significant horizontal flow occurs in the top layer. Maximum ages of about 40 years occur near the left end of the discharge region, and these ages are similar to the ages in the previous simulation at the same location. For this location, the main control on the age is the time spent in the top layer, and that has not changed because the porosity of the top layer, and of course the specific discharge everywhere, is identical to the previous simulation.

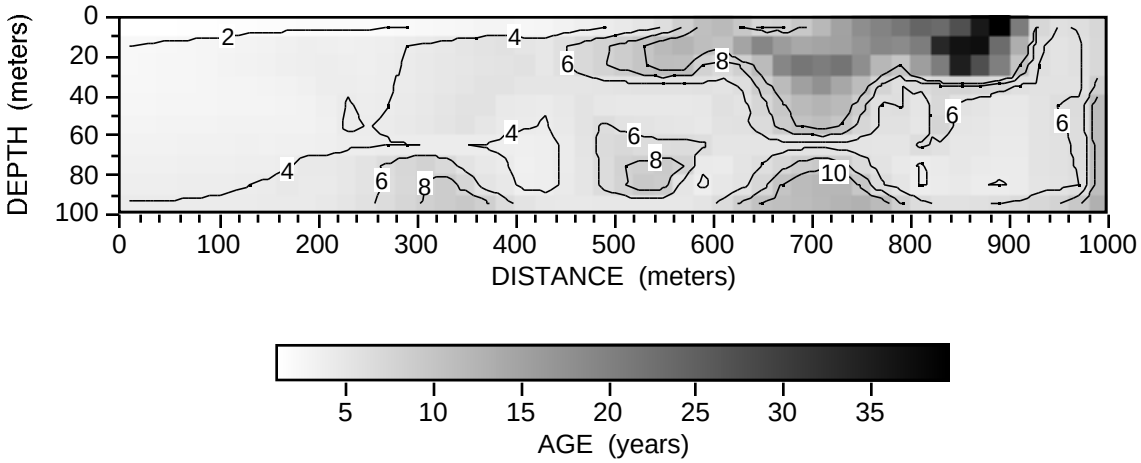

Figure 2-8 Results of direct simulation of groundwater age in a cross-section through a **stratified heterogeneous** regional aquifer system in which eight discontinuous high-permeability zones occur at three different depths. Each zone is 10 m thick with hydraulic conductivity 10^{-4} m/s and with horizontal extent of 200 m. The remainder of the aquifer system has hydraulic conductivity 10^{-6} m/s. Porosity is θ=0.2 in the upper 10 m and is θ_2=0.01 in the remainder of the aquifer. (Streamlines are the same as fig. 2-7a) Contours of simulated groundwater age for advection only ($D_m = \alpha_L = \alpha_T = 0$). Contour interval 10 years.

In summary, these regional cross-section examples illustrate the utility of the method of direct simulation of ground-water age, and the complexity in spatial age patterns that can be created by heterogeneities in hydraulic conductivity and porosity. The methods presented here for direct simulation of ground-water facilitate computation of age throughout an aquifer with simple modifications to existing solute transport models. Although environmental tracers offer additional information, compared to hydraulic head measurements, it may not be easy to unravel the underlying permeability distribution from spatially variable age distributions; highly complex age patterns emerge from relatively simple simulations, albeit ones with at least one order of magnitude variability in permeability.

2.3.2 Matrix Diffusion from a Single Fracture

Matrix diffusion can be an important aspect of transport of solutes in ground water, particularly in fractured-rock settings. Matrix diffusion generally refers to diffusive exchange between high-permeability fractures or fracture zones and low-permeability rock *matrix*, whether much less fractured or unfractured. Water flow occurs primarily in the fractures and flow is often modeled ignoring the permeability of the rock matrix. However, diffusive exchange of solutes between the flowing water in the fractures and the immobile water in the rock matrix can have significant impacts on solute migration (Grisak and Pickens, 1980; Sudicky and Frind, 1982).

The impact of matrix diffusion on age transport is examined here for a one-dimensional flow system using MOC3D (Goode and Konikow, 1991; Konikow and others, 1996) modified to solve the transient age transport equation (2.10). A 1 m long column is discretized with 10 cells ($\Delta x = 0.1$ m). Imposed fixed-head boundary conditions yield a specific discharge of 1 m/day, and the porosity of 0.01 results in a uniform velocity of 100 m/day. This porosity represents the high-permeability fractures in the rock column. Ignoring dispersion and matrix diffusion, the steady-state age at a x = 9.5 m is simply the travel time: A (x=9.5) = x / V = 9.5 m / 100 m/day = 0.095 day.

At steady state, the effect of matrix diffusion is an apparent increase in porosity, from that of the fractures alone, to the sum of both fracture and matrix porosity (θ_m ; eq. 2.15). In this case, the apparent travel time to x = 9.5 m, and the steady-state age, is A = x / [q/(θ + θ_m)] = 9.5 m / [1 m/day / (0.01 + 0.09)] = 0.95 day, or an increase by an order-of-magnitude. This increase corresponds directly to the increase in porosity from 0.01 to 0.10. However, the rate at which this steady state is approached depends on the system properties.

The exchange of age-mass between the fractures and the rock matrix is the term F in the governing equation (2.10). In the rock matrix, the age transport processes are limited to accumulation, production, and diffusion. Diffusion is assumed to be one-dimensional in the rock matrix, orthogonal to fractures. An integral balance equation for age-mass in the rock matrix is

$$\frac{d A_m}{dt} = 1 - \frac{\beta \left(A_m - A\right)}{\theta_m} \quad . \tag{2.16}$$

where A_m is the average age in the rock matrix, A is the age in the fracture system at the same location, β [T^{-1}] is a linear exchange coefficient characterizing diffusion between the fracture and the rock matrix, and the density is assumed to be constant. The term F in the fracture governing equation is F = $\rho\beta$ (A_m - A) and corresponds to the age-mass flux into the fractures per unit volume of aquifer.

The linear exchange coefficient is generally proportional to the diffusion coefficient (D_m) divided by a characteristic length (b) squared:

$$\beta \propto \frac{D_m}{b^2} \quad . \tag{2.17}$$

For example, for the case of planar fractures, the linear exchange coefficient corresponding to a 1-node finite-difference approximation is given by:

$$\beta = \frac{1}{2}\frac{D_m}{b^2} \quad . \tag{2.18}$$

where b is the block half-thickness. This simple linear model of matrix diffusion is strictly accurate only for relatively small diffusion distances, i.e. small b. However, this kinetic exchange model can be considered a first-order approximation of the impact of exchange between high-permeability and much lower-permeability portions of a flow system, whether limited strictly to diffusion or not.

The initial age is assumed to be zero throughout the aquifer. At early time, water at all locations ages as simulation time progresses (fig. 2-9). If the linear exchange coefficient is low ($\beta = 10^{-4}$ m^2/day in fig. 2-9), then the age temporarily stabilizes at a level corresponding to the travel time in the fractures alone, 0.095 day. However, eventually the age in the matrix builds up to such high levels that the age-mass flux into the fracture is sufficient to increase the age in the fractures, and eventually reach a new plateau corresponding to the travel time computed from the total porosity, 0.95 day. The magnitude of the linear exchange coefficient (β) controls the time at which matrix diffusion has a significant impact on computed ages. For very high β, the initial plateau is not present because the fracture and matrix ages are essentially in equilibrium at all times (fig. 2-9).

Equation (2.16) can be used to compute the steady-state age in the rock matrix from the steady-state age in the fracture: $A_m = A + \theta_m / \beta$. Hence for this case the steady-state ages in the matrix at x = 9.5 m for $\beta = 1, 10^{-2}$, and 10^{-4} day^{-1} are $A_m = 0.185$, 9.095 and 900.095 days., respectively.

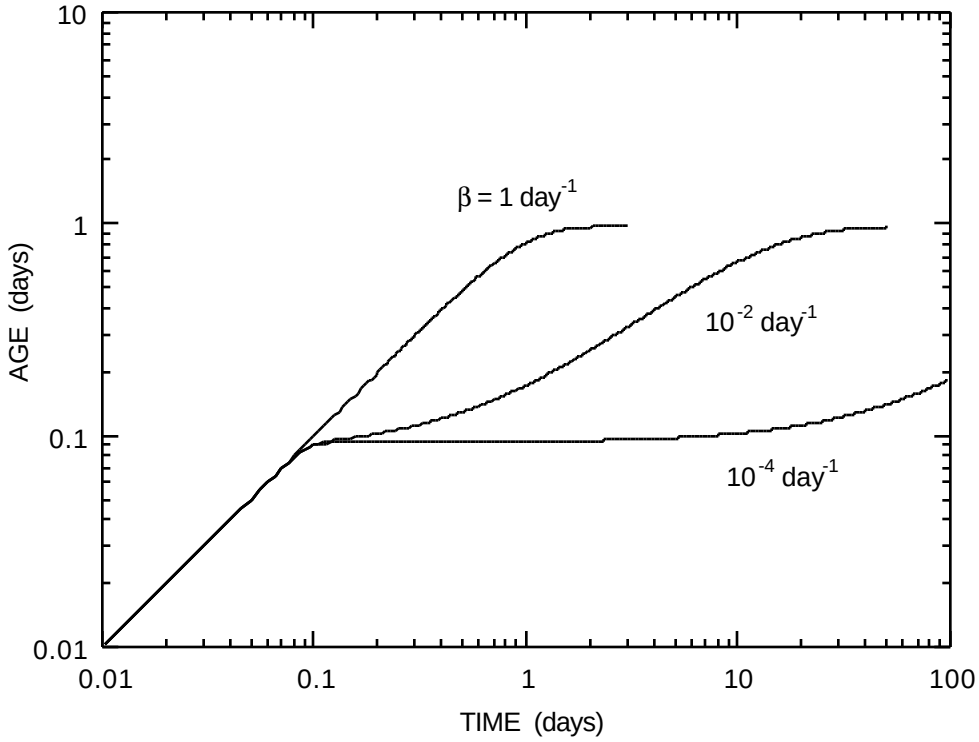

Figure 2-9 Age at x = 9.5 m from the inflow boundary of a one-dimensional rock column having fracture porosity 0.01, rock matrix porosity 0.09, and specific discharge 1 m/day. The initial condition is age = 0 at all locations. Age is shown as a function of simulation time for three values of linear exchange coefficient (β) characterizing the rate of mass transfer by diffusion between the flowing water in the fractures and the immobile water in the rock matrix.

2.3.3 Age of Pumped Samples from a Heterogeneous Formation

The age in a ground-water system can be estimated from concentrations of environmental tracers in samples pumped from wells. For example, the time since water has been isolated from the atmosphere can be estimated from CFC concentrations because the atmospheric concentration has been increasing for about the last 50 years (Plummer et al., 1993). When drawing water from a well, particularly one with a long screened or open interval, the pumped water is a mixture of water from different parts of the aquifer. This mixing can significantly complicate or add uncertainty to estimation of

ground-water age. Furthermore, the age of discharging water after a pump is turned on would change in time as water from a larger and larger capture volume enters the well.

A hypothetical simulation illustrates use of the direct age method to model the time-evolution of age in water discharging from a pumping well in a highly heterogeneous formation. This simulation is based on a well-field scale model developed by Paul Hsieh (USGS, Menlo Park, California, written communication, 1994) of ground-water flow during an aquifer test in fractured rock at Mirror Lake NH. Aquifer hydraulic properties (Table 2-1) were estimated by calibrating steady-state and transient models of three-dimensional flow during the test. These properties are used here in a model of both steady-state age distribution and age transport during pumping tests.

Table 2-1. Hydraulic Properties of Three-Dimensional Model of Highly-Heterogeneous Formation (Paul A. Hsieh, U.S. Geological Survey, written communication, 1994).

		Hydraulic Conductivity (m/s)	
Hydrogeologic Unit	Model Layers	Horizontal	Vertical
Overburden	1-5	1.8×10^{-6}	1.8×10^{-6}
Bedrock Surface	between 5 & 6	--	1.9×10^{-8}
Highly-Fractured	parts of 11, 22 & 38	5.6×10^{-5}	--
Less-Fractured	6-38	3.3×10^{-8}	1.9×10^{-7}

The model grid is 22 rows x 14 columns x 38 layers. The grid spacing is uniform throughout the grid with $\Delta x = \Delta y = 7.62$ m, $\Delta z = 1.5$ m. The highly-fractured zones of the bedrock are simulated as 1.5 m thick porous media units with much higher hydraulic conductivity than the surrounding bedrock (fig. 2-x).

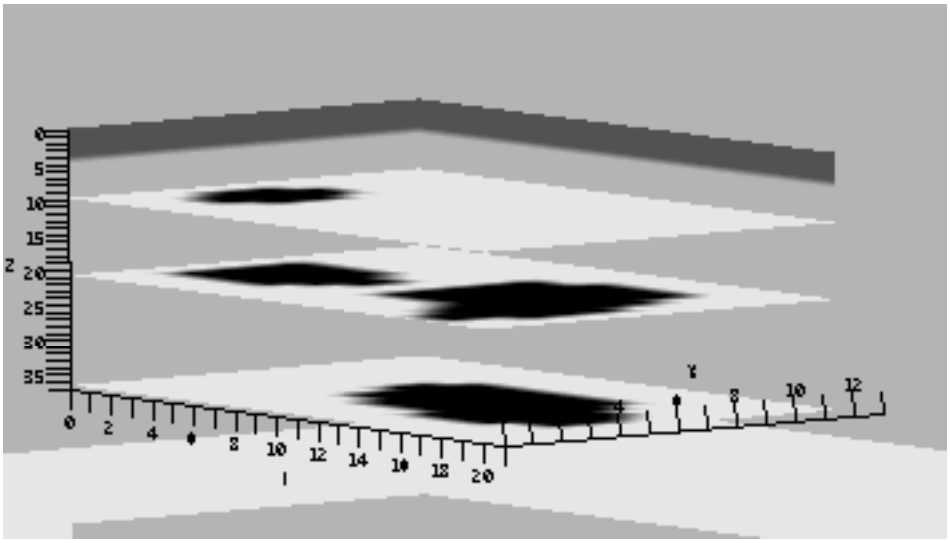

Figure 2-10 Hydraulic conductivity distribution for three-dimensional highly-heterogeneous case. Weathered zone at top (dark gray) has K = 2.7 x 10^{-6} m/s; four horizontal highly-fractured zones (black) occur at three different depths and have K = 8.4 x 10^{-5} m/s; the remainder of the less-fractured bedrock has K = 5 x 10^{-8} m/s.

The initial steady-state distribution of ground-water age is assumed to represent conditions prior to pumping. The average annual recharge of 368 mm/yr is distributed over the top of the model. All other boundaries are no-flow, except the face at y = 168 m where the head in all model layers is fixed at 0.0. Age is simulated only in the bedrock portion of the aquifer and it is assumed that all water inflowing from the overburden has age zero. For advection alone, the age distribution is efficiently computed using particle tracking and equation (2.1). For the age simulation, the bedrock porosity is assumed to be 0.001, which corresponds to a bulk porosity of fracture volume per unit volume of rock.

Maximum ages occur at the bottom of the system where less-fracture bedrock underlies the highly-fractured zones (fig. 2-11; fig. 2-12). Flow is generally downward from the overburden into the horizontal fracture zones, and then laterally out along the downgradient face (front face in fig. 2-11; right end of cross-section in fig 2-12 (a)). The fracture zone at the bottom of the model is shown as the area of blue age in fig. 2-11.

The maximum ages are diluted downgradient from the red area by much younger waters in the fracture flow system. Resulting outflow face ages are high only at the very bottom of the aquifer (fig. 2-12(b)).

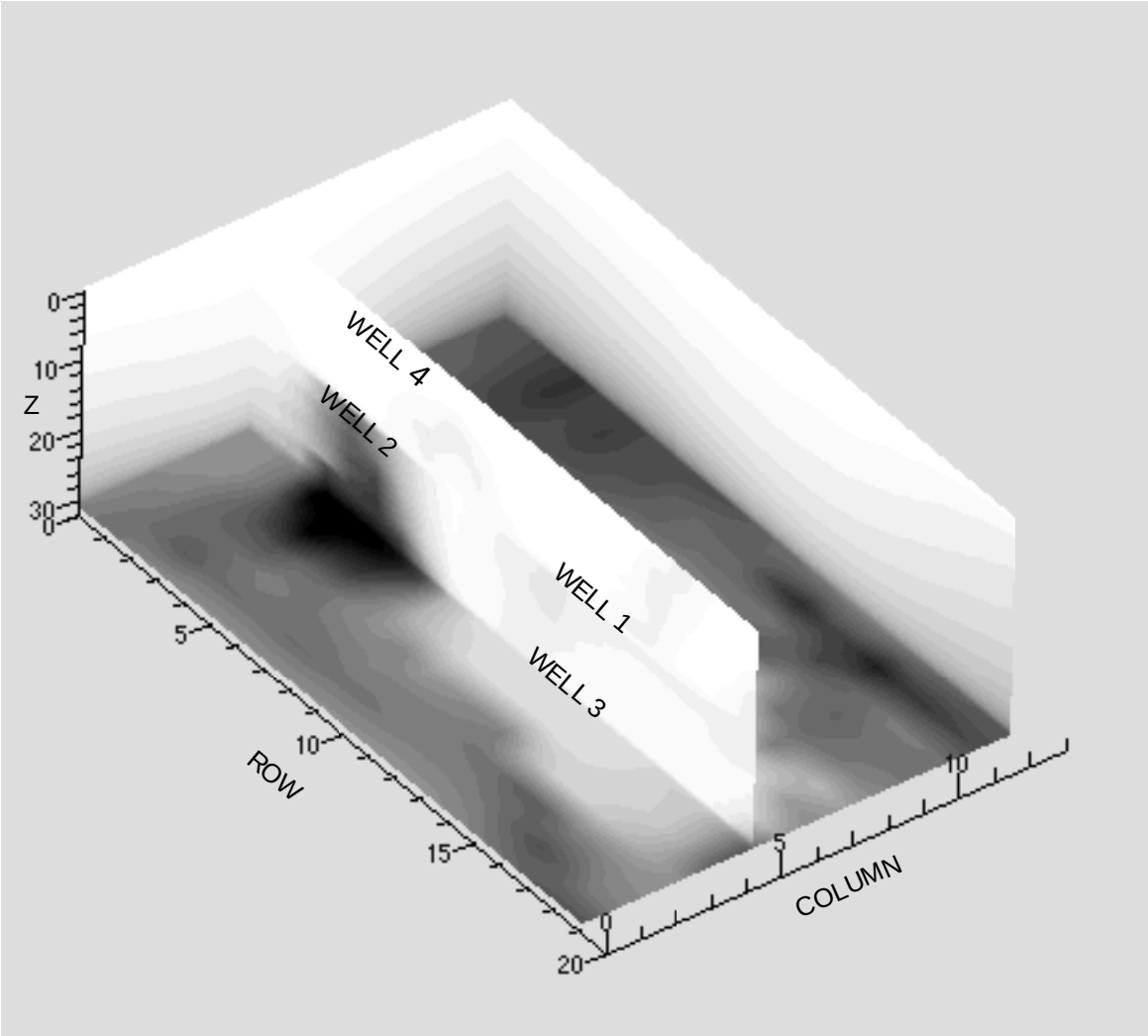

Figure 2-11 Results of direct simulation of steady-state groundwater age in a highly-heterogeneous fractured bedrock. Hydraulic properties are shown in fig. 2-10 and summarized in table 2-1. Also shown are locations of wells which are not pumping in this simulation. The colors correspond to age, ranging from less than 3 years (white) to greater than 700 years (black).

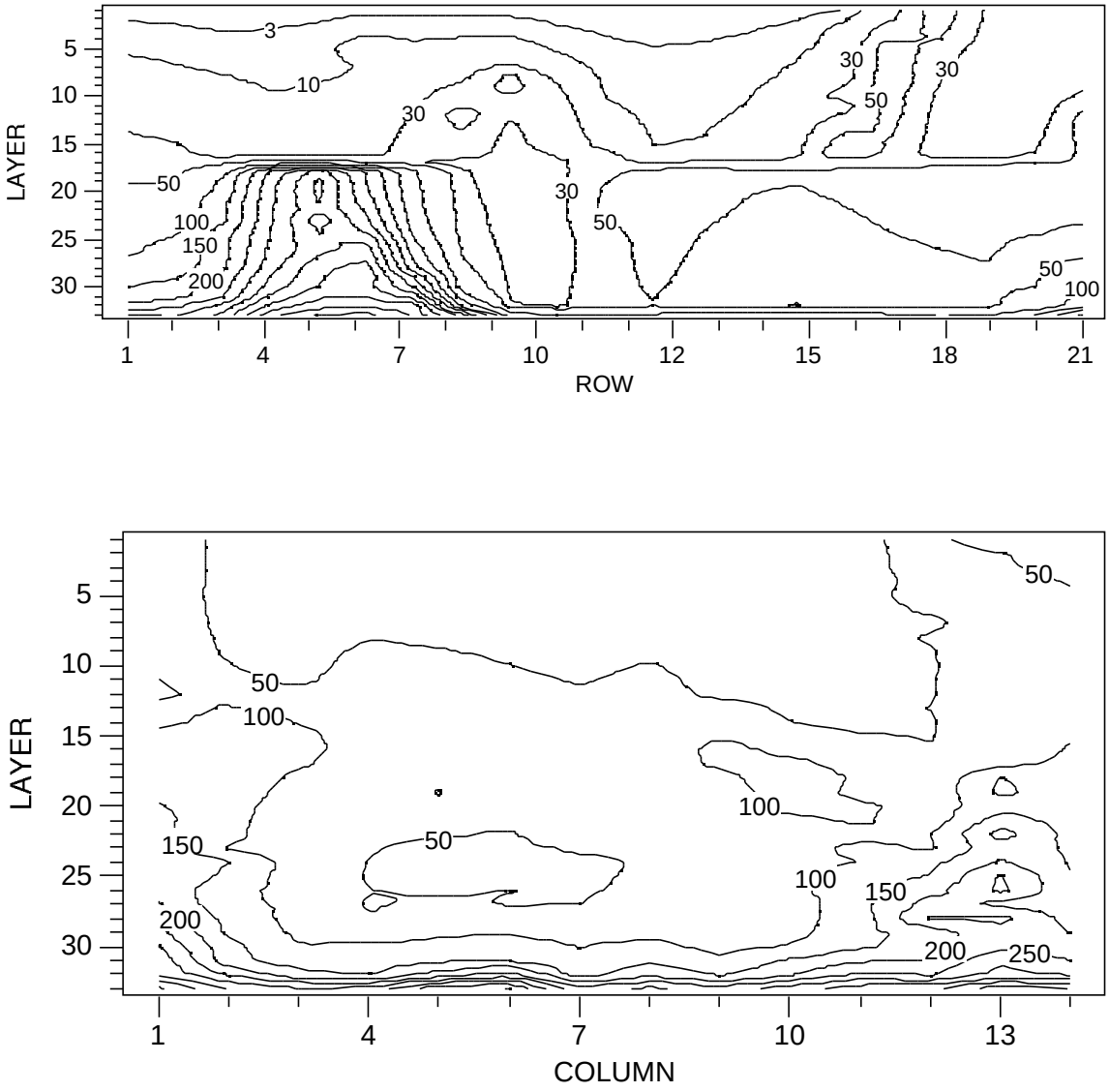

Figure 2-12 Results of direct simulation of steady-state groundwater age in a highly-heterogeneous fractured bedrock. Hydraulic properties are shown in fig. 2-10 and summarized in table 2-1. (a) Y-Z cross-section along the middle of the model at column 7 (x=53 m), variable contour intervals in years. (b) X-Z cross-section at the outflow end of the model along row 21 (y=160 m), contour intervals are 50 years.

Ground-water age in pumped samples is evaluated for four fracture-zone well locations. In each case, the initial age distribution is that from the previous steady-state age simulation. A steady-state flow field is generated for each pumping scenario by imposing no-flow boundaries on the model bottom and all four sides. The top layer of the overburden is modeled as a fixed-head boundary from which all of the flow to the well is ultimately derived. Each well is pumped separately at a rate of 10.6 L/min.

The evolution of ground-water age of pumped samples is different for each well (fig. 2-13). Wells 1 and 2 are in downgradient and upgradient fracture zones near mid-depth in the model. Age in downgradient well 1 increases sharply at early time from about 37 years to over 40 years, levels off near 43 years, and appears to be gradually increasing after 10 hours of pumping. Well 2 is in the upgradient fracture zone at the same depth, and its age is initially higher. Age in well 2 drops, but not as sharply in time, from 54 years to less than 46 years and then increases to about 56 years at the end of the simulation. The small-scale fluctuations in the age are numerical artifacts of the discrete method-of-characteristics model (Konikow and other, 1996).

Ground-water age in samples from wells 3 and 4 decrease logrithmically in time from the initial values (fig. 2-13). Well 3 is located (fig. 2-11) in the bottom fracture zone and has the highest initial age, over 200 years. However, the age decreases sharply to less than 120 years after 2 hours of pumping and is less than 100 years after 10 hours. Well 4 shows a similar pattern, but at much younger ages. This well is located in the top fracture zone, much closer to the recharge source in the overburden. Ages in samples from well 4 decrease from over 12.5 years initially to less than 8.5 years after 10 hours.

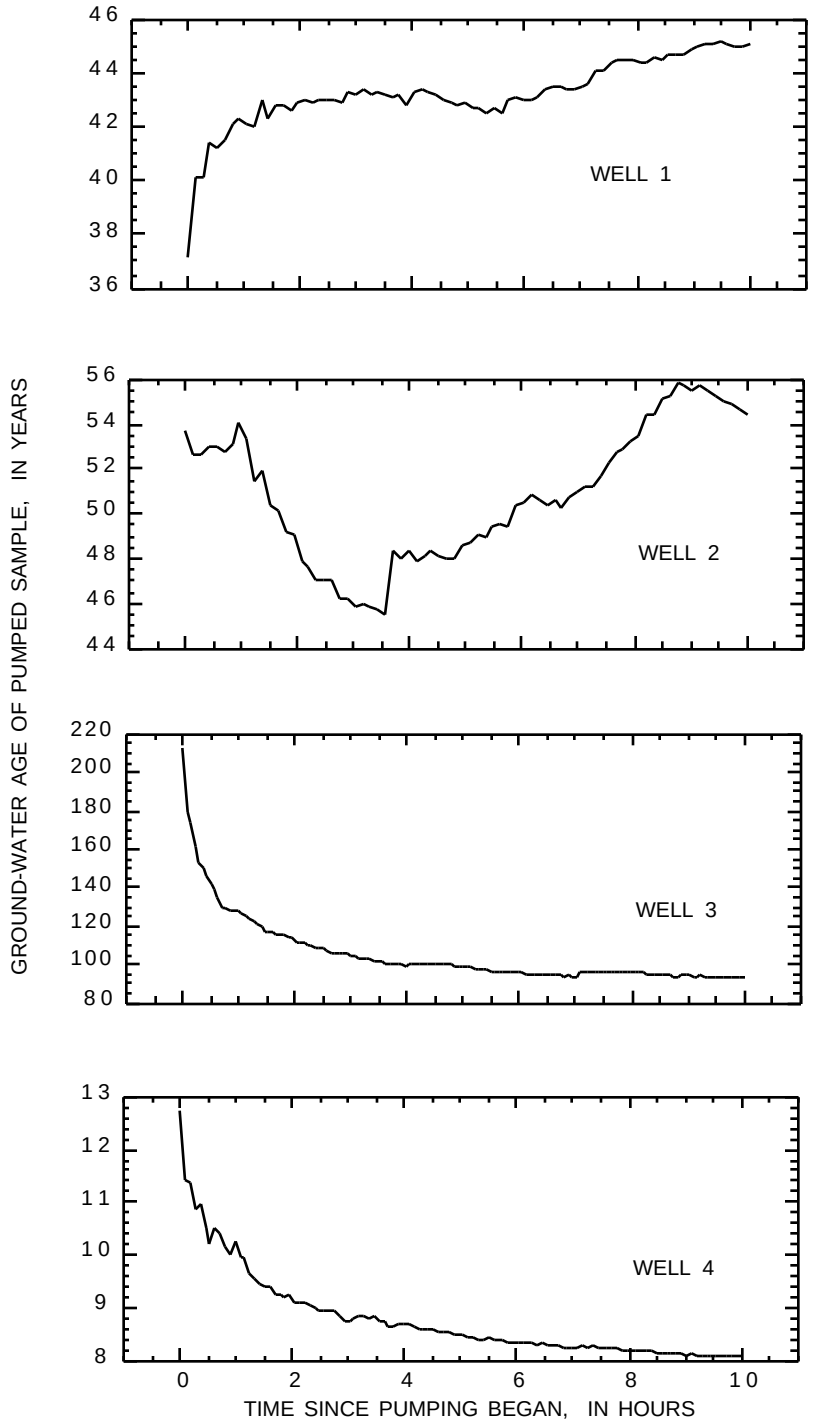

Figure 2-13 Sample age as a function of pumping time in a highly-heterogeneous aquifer. Age transport to the pumping well is simulated with four different steady-state flow models having only the well of interest pumping. The initial age distribution for each case is the steady-state age shown in fig. 2-11. Hydraulic properties are shown in fig. 2-10 and summarized in table 2-1. Locations for each well are shown in fig. 2-11.

2.3.4 Two-Dimensional Age Distribution in Mildly-Heterogeneous Porous Media

Simulation of the age distribution in a hypothetical aquifer illustrates features of ground-water age in relatively homogeneous systems. Intensive field tracer experiments have been conducted at a military reservation on Cape Cod, Massachusetts. LeBlanc and others (1991) describe a natural gradient tracer test conducted over 2 years using nonreactive and reactive tracers in a relatively homogeneous sand and gravel aquifer. Garabedian and others (1991) analyze the spreading of a nonreactive tracer and estimate asymptotic dispersivities from the temporal growth in the spatial moments of the tracer distribution. Hess and others (1992) compare field and laboratory measurements of hydraulic conductivity and estimate macrodispersivities from theoretical relations.

A hypothetical two-dimensional aquifer is generated that has heterogeneous hydraulic conductivity with spatial statistics similar to those from the Cape Cod tracer test. The turning bands methods (Mantoglou and Wilson, 1982; Zimmerman and Wilson, 1989) is used to generate a spatially correlated field of hydraulic conductivity (K). K is assumed to be lognormally distributed with mean 110 m/d (Garabedian et al., 1991) and variance of the natural log of K = 0.24 (Hess et al., 1992). An exponential spatial covariance function is assumed with zero nugget and isotropic correlation length of 2.6 m (Hess et al., 1992). The grid is 100 m by 20 m and is discretized by 500 x 100 square blocks having $\Delta x = \Delta y = 0.2$ m. The single realization of K used (fig. 2-14a) reflects the underlying statistical properties: most of the K values are clustered near and below the mean value, the size of the high and low zones are larger than individual grid blocks and smaller than the grid dimensions; only a few isolated zones exhibit K > 300 m/d.

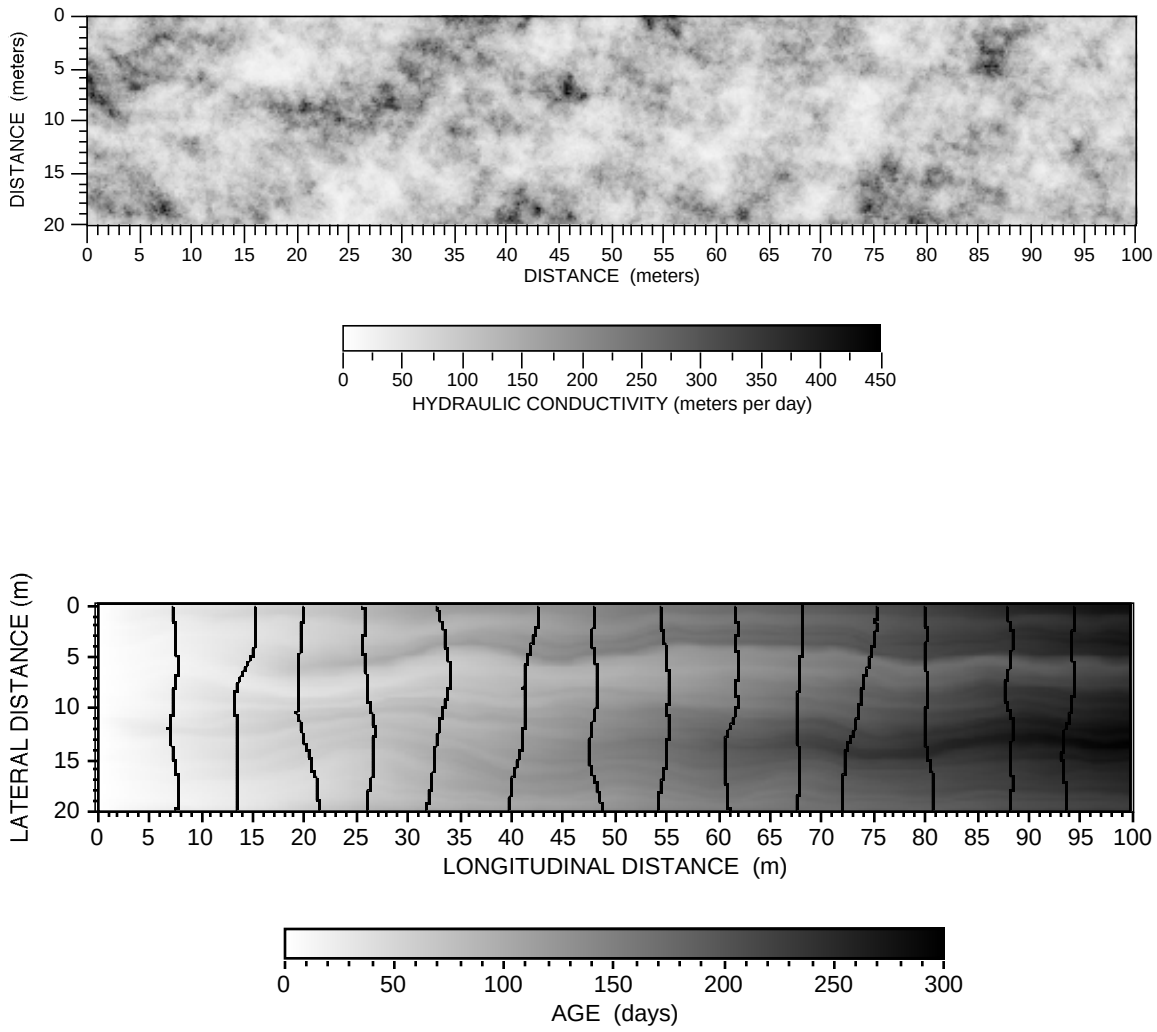

Figure 2-14 Age simulation in a mildly heterogeneous two-dimensional aquifer: (a) Hydraulic conductivity distribution; (b) Hydraulic head contours (0.01 m interval) and age distribution for advection-only.

The boundary conditions for the steady-state flow model are h(x=0) = 0.148 m; h(x=100 m) = 0 m; and no-flow at y = 0 and y = 20 m. These boundary conditions, along with an assumed porosity of 0.39 (LeBlanc et al, 1991) yield an average velocity of about 0.4 m/d.

The steady-state age distribution (fig. 2-14b) is more variable than the head distribution and indicates significant persistence of thin ‘fingers’ of contrasting age.

Youngest ages occur along a somewhat continuous zone of elevated K in the upper half (y<10m) of the aquifer. However, an adjacent zone with older water reflects the impact of a large zone of low K located at about (x,y)=(20m,5m). The resulting large difference in age between closely space streamlines persists downstream to the end of the aquifer. This 'slip' between adjacent streamlines would be modeled as longitudinal dispersion if the small-scale K variability were not explicitly accounted for.

The spatial variability of the steady-state age distribution can also be illustrated by plots of age as a function of distance. In the longitudinal direction, the age generally increases more or less smoothly in the average direction of flow (fig. 2-15a). For much of the domain, the variability in the x-direction is relatively smooth, as illustrated by the lines at y = 7.3 and 13.3 m. The overall rate of increase in age versus x shown for these two lines essentially brackets all longitudinal transects in this simulation. Significantly more variability along x is illustrated near the position of the large low-K zone, as shown by the line at y = 5.3 m. At this position, the age does not monotonically increase in the mean direction of flow. For example, the water at (x,y) = (45m,5.3m) is about 30 days older than water 5 m further down (the mean) gradient at (x,y) = (50m,5.3m). Close examination of other lines indicates that in this simulation all lines have portions where age decreases in the mean flow direction. This decrease in age in the mean flow direction is due to the difference between the actual streamlines and the mean path.

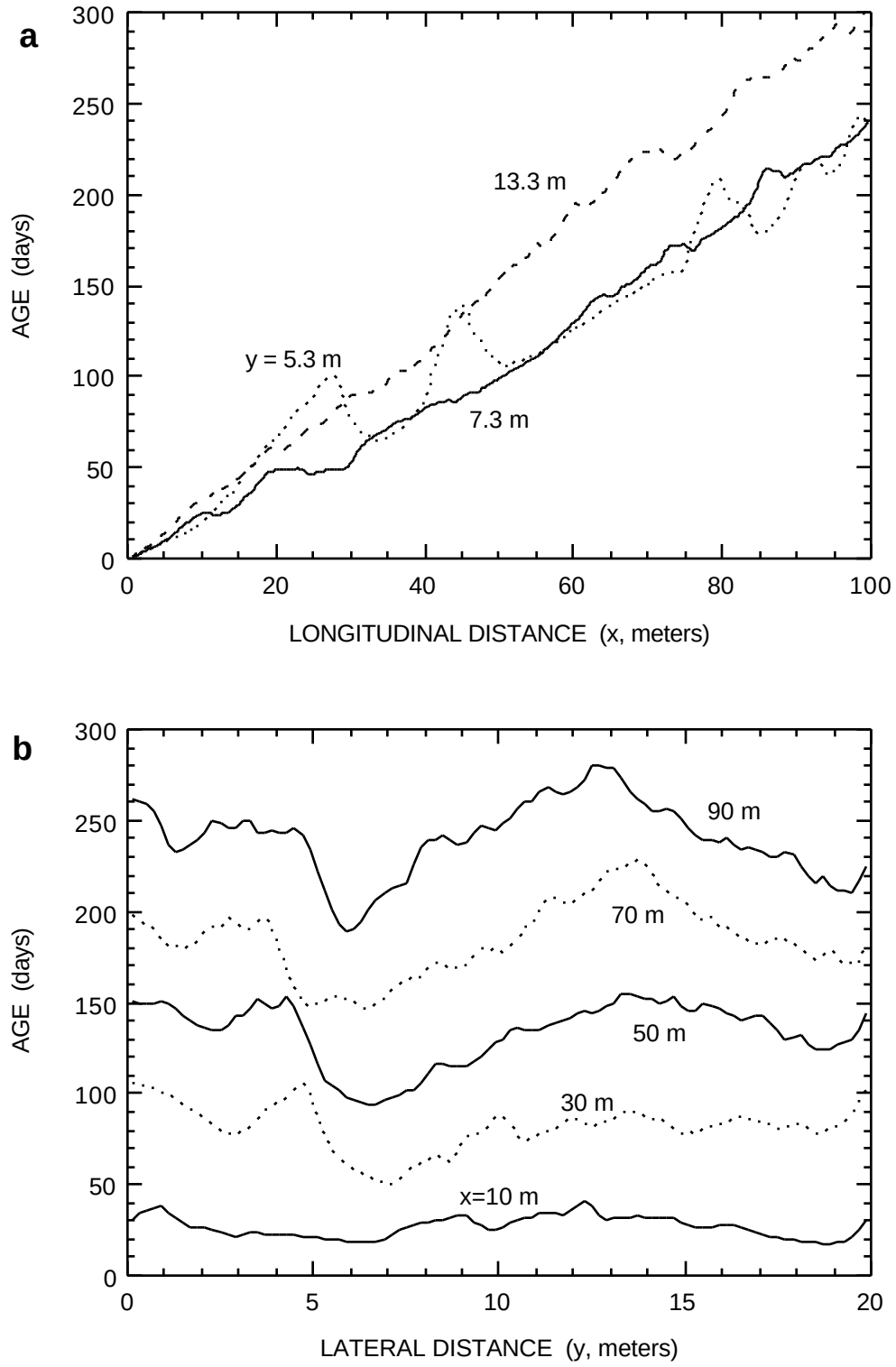

Figure 2-15 Age variation along lines oriented longitudinal (a) and lateral (b) to the average flow direction for a mildly heterogeneous two-dimensional aquifer.

Variability in age is pronounced in the y-direction, lateral or transverse to the mean flow direction (fig. 2-15b). The variability is less at the upstream boundary because by definition the age is uniform at 0 days at x=0. A significant peak of older water develops between x = 10 and 30 m because of the large low-K zone discussed above. Although the y position of this peak shifts due to shifting flowlines, the magnitude of the difference between the age on this peak and on adjacent streamlines persists through the simulated domain.

2.4 Summary

A new method is developed to simulate groundwater age. The spatial distribution of groundwater age is governed by a transport equation that has an internal source of unit (1) strength, corresponding to the rate of aging. This governing equation is derived both from residence-time-distribution concepts, and from mass-conservation principles applied to conceptual age mass. This method of groundwater age simulation falls between existing approaches of, on one hand, simulation of groundwater age as governed by advection alone, by using a particle tracking model and, on the other hand, simulation of isotopes or chemical markers of interest in a solute transport model. Use of the theory presented here allows general simulation of groundwater age, without solute-specific modeling, by incorporating the physical effects of diffusion, dispersion, mixing, and exchange processes on age. These methods can be incorporated easily in existing models of transport in aquifers.

Application of this theory is illustrated for several examples. The impact of layered heterogeneity on regional scale age distribution is examined in cross-section for cases with and without dispersion and diffusion. Average ages are not highest at the discharge boundary in many cases, and the shadowing effect of high-permeability units on gradients in surrounding low-permeability units is illustrated. Matrix diffusion causes a ‘retardation’ of apparent velocity at steady state, but the rate at which steady state is approached may be slow, as controlled by diffusion in the rock matrix. The age transport equation is a convenient method of examining the time variation of age of pumped samples. For the case examined, the time history of age of pumped samples depends on the local conditions near the well and may result in large changes in age during pumping at some locations. Finally, a relatively homogeneous example illustrates that even when the spatial variability of hydraulic conductivity is relatively small, the age distribution is not smooth. The age is much more sensitive to variability in K than the head. Hence,

deviation of age from the mean value can provide significant information about heterogeneity. On the other hand, interpretation of mean age from a limited number of point samples is complicated by this sensitivity.

2.5 References

Bair, E. S., R.A. Sheets, and S.M. Eberts, Particle-tracking analysis of flow paths and travel times from hypothetical spill sites within the capture area of a wellfield, Ground Water, 28(6), 884-892, 1990.

Bear, J., *Hydraulics of Groundwater*, McGraw-Hill, New York, 1979.

Bolin, B., and Henning Rodhe, A note on the concepts of age distribution and transit time in natural reservoirs, Tellus, 25(1), 58-62, 1973.

Campana, M. E., and E.S. Simpson, Groundwater residence times and recharge rates using a discrete-state compartment model and 14C data, J. Hydrol., 72, 171-185, 1984.

Dagan, G., and V. Nguyen, A comparison of travel time and concentration approaches to modeling transport by groundwater, J. Contaminant Hydrology, 4, 79-91, 1989.

Danckwerts, P. V., Continuous flow systems: Distribution of residence times, Chemical Eng. Sci., 2, 1-13, 1953.

Egboka, B. C. E., J.A. Cherry, R.N. Farvolden, and E.O. Frind, Migration of contaminants in groundwater at a landfill: A case study, 3, Tritium as an indicator of dispersion and recharge, J. Hydrol., 63, 51-80, 1983.

Eriksson, E., The possible use of tritium for estimating groundwater storage, Tellus, 10(4), 472-478, 1958.

Freeze, R.A., and J.A. Cherry, *Groundwater*, Prentice-Hall, Englewood Cliffs, New Jersey, 1979.

Freeze, R. A., and P.A. Witherspoon, Theoretical analysis of regional groundwater flow. 2. Effect of water-table configuration and subsurface permeability variation, Water Resour. Res., 3(2), 623-634, 1967.

Fritz, P., J.E. Gale, and E.J. Reardon, Comments on carbon-14 dating of groundwaters in crystalline environments, Geoscience Canada, 6(1), 10-15, 1979.

Garabedian, S.P., D.R. LeBlanc, L.W. Gelhar, and M.A. Celia, 1991, Large-scale natural gradient tracer test in sand and gravel, Cape Cod, Massachusetts 2. Analysis of spatial moments for a nonreactive tracer: Water Resources Research, v. 27, no. 5, p. 911-924.

Geyh, M. A., and G. Backhaus, Hydrodynamic aspects of carbon-14 groundwater dating, in *Isotope Hydrology 1978*, v. 2, pp. 631-643, International Atomic Energy Agency, Vienna, 1978.

Goode, D. J., Particle velocity interpolation in block-centered finite difference groundwater flow models, Water Resour. Res., 26(5), 925-940, 1990.

Goode, D.J., Direct simulation of groundwater age: Water Resources Research, 32(2), 289-296, 1996.

Goode, D. J., and L. F. Konikow, Testing a method-of-characteristics model of three-dimensional solute transport in ground water, in Proc. *Symposium on Ground Water*, Nashville, Tenn., July 29–August 2, 1991, edited by G.P. Lennon, pp. 21-27, Am. Soc. Civ. Eng., New York, 1991.

Grisak, G.E., and J.F. Pickens, 1980, Solute transport through fractured media, 1, The effect of matrix diffusion: Water Resources Research, 16, 719-730.

Harvey, C.F., and S.M. Gorelick, Moment generating equations: Modeling transport and mass transfer in heterogeneous aquifers, Water Resour. Res., 31(8), 1895-1911, 1995.

Hess, K.M., S.H. Wolf, and M.A. Celia, Large-scale natural gradient tracer test in sand and gravel, Cape Cod, Massachusetts 3. Hydraulic conductivity variability and calculated macrodispersivities: Water Resources Research, 28(8), 2011-2027, 1992.

Kinzelbach, W., The random walk method in pollutant transport simulation, in *Groundwater Flow and Modeling*, edited by E. Custodio et al., pp. 227-245, D. Reidel, Hingham, Mass., 1988.

Konikow, L.F., and D.B. Grove, Derivation of equations describing solute transport in ground water, U.S. Geological Survey Water-Resources Investigations Report 77-19, 1977.

Konikow, L.F., D.J. Goode and G.Z. Hornberger, A three-dimensional method-of-characteristics solute-transport model (MOC3D): U.S. Geological Survey Water-Resources Investigations Report 96-4267, 87 p., 1996.

Kreft, A., and A. Zuber, On the physical meaning of the dispersion equation and its solutions for different initial and boundary conditions, Chemical Eng. Sci., 1471-1780, 1978.

LeBlanc, D.R., S.P. Garabedian, K.M. Hess, L.W. Gelhar, R.D. Quadri, K.G. Stollenwerk, and W.W. Wood, Large-scale natural gradient tracer test in sand and gravel, Cape Cod, Massachusetts 1. Experimental design and observed tracer movement: Water Resources Research, 2( )5, 895-910, 1991.

Lee, S.-I., and P.K. Kitanidis, Analysis of groundwater flow and travel times for a landfill site in an arid region with a thick vadose zone, Hydrological Processes, 7, 373-387, 1993.

Levenspiel, O., *Chemical Reaction Engineering*, Wiley, New York, 1972.

MacMullin, R. B., and M. Weber, Jr., The theory of short-circuiting in continuous-flow mixing vessels in series and kinetics of chemical reactions in such systems, Transactions of American Institute of Chemical Engineers, 31(2), 409-458, 1935.

Mantoglou, A., and J.L. Wilson, The turning bands method for simulation of random fields using line generation by a spectral method: Water Resources Research, 18(5), 1379-1394, 1982.

Maloszewski, P., and Andrzej Zuber, Influence of matrix diffusion and exchange reactions on radiocarbon ages in fissured carbonate aquifers, Water Resour. Res., 27(8), 1937-1945, 1991.

Mazor, E., and Ronit Nativ, Hydraulic calculation of groundwater flow velocity and age: Examination of the basic premises, J. Hydrol., 138, 211-222, 1992.

McDonald, M.G., and A.W. Harbaugh, A modular three-dimensional finite-difference ground-water flow model, U.S. Geological Survey Techniques of Water-Resources Investigations, book 6, chapter A1, 1988.

Musgrove, M., and J.L. Banner, Regional ground-water mixing and the origin of saline fluids: Midcontinent, United States, Science, 259, 1877-1882, 1993.

Nauman, E. B., Residence time distributions in systems governed by the dispersion equation, Chemical Eng. Sci., 36, 957-966, 1981.

Nir, A., On the interpretation of tritium 'age' measurements of groundwater, J. Geophys. Res., 69(12), 2589-2595, 1964.

Nir, A., and S. Lewis, On tracer theory in geophysical systems in the steady and non-steady state, Part I, Tellus, 27(4), 372-383, 1975.

Plummer, L. N., R.L. Michel, E.M. Thurman, and P.D. Glynn,. Environmental tracers for age dating young ground water, in *Regional Ground-Water Quality* , edited by W. M. Alley, pp. 255-294, Van Nostrand Reinhold, New York, 1993.

Reilly, T. E., L.N. Plummer, P.J. Phillips, and E. Busenberg, The use of simulation and multiple environmental tracers to quantify flow in a shallow aquifer, Water Resour. Res., 30(2), 421-433, 1994.

Robinson, B. A., and J.W. Tester, Dispersed fluid flow in fractured reservoirs: An analysis of tracer-determined residence time distributions, J. Geophys. Res., 89(B12), 10374-10384, 1984.

Sandberg, M., What is ventilation efficiency?, Building and Environment, 16(2), 123-135, 1981.

Shapiro, A. M., and V.D. Cvetkovic, Stochastic analysis of solute arrival time in heterogeneous porous media, Water Resour. Res., 24(10), 1711-1718, 1988.

Simpkins, W. W., and K. R. Bradbury, Groundwater flow, velocity, and age in a thick, fine-grained till unit in southeastern Wisconsin, J. Hydrol., 132, 283-319, 1992.

Solomon, D. K., S.L. Schiff, R.J. Poreda, and W.B. Clarke, A validation of the 3H/3He method for determining groundwater recharge, Water Resour. Res., 29(9), 2951-2962, 1993.

Spalding, D. B., A note on mean residence-times in steady flows of arbitrary complexity, Chemical Eng. Sci., 9, 74-77, 1958.

Sudicky, E. A., and E.O. Frind, Carbon 14 dating of groundwater in confined aquifers: Implications of aquitard diffusion, Water Resour. Res., 17(4), 1060-1064, 1981.

Sudicky, E.A., and E.O. Frind, Contaminant transport in fractured porous media: Analytical solutions for a system of parallel fractures: Water Resources Research, 18, 1634-1642, 1982.

Torgersen, T., W.B. Clarke, and W.J. Jenkins, The tritium/helium-3 method in hydrology, in *Isotope Hydrology 1978*, pp. 917-930 , International Atomic Energy Agency, 1978.

Walker, G. R., and P.G. Cook, The importance of considering diffusion when using carbon-14 to estimate groundwater recharge to an unconfined aquifer, J. Hydrol., 128, 41-48, 1991.

Weeks, E. P., D.E. Earp, and G.M. Thompson, Use of atmospheric fluorocarbons F-11 and F-12 to determine the diffusion parameters of the unsaturated zone in the southern high plains of Texas, Water Resour. Res., 18(5), 1365-1378, 1982.

Wen, C. Y., and L.T. Fan, *Models for Flow Systems and Chemical Reactors*, Marcell Decker, New York, 1975.

Zimmerman, D.A., and Wilson, J.L., Description and user's manual for TUBA: A computer code for generating two-dimensional random fields via the turning bands method: unpublished report, Geosci. Dep., N.M. Inst. of Min. and Technol., Socorro, 1989.

Zuber, A., Mathematical models for the interpretation of environmental radioisotopes in groundwater systems, in *Handbook of Environmental Isotope Geochemistry*, edited by P. Fritz and J. Ch. Fontes, pp. 1-59, Elsevier, Amsterdam, 1986.